

# Constraining Airborne Electromagnetic Interpretation with Regolith Stratigraphy and Landscape Evolution Processes

**Andrew King\***

CSIRO

26 Dick Perry Ave, Kensington WA 6151

Andrew.King@csiro.au

**Ignacio Gonzalez-Alvarez**

CSIRO

26 Dick Perry Ave, Kensington WA 6151

Ignacio.Gonzalez-Alvarez@csiro.au

## SUMMARY

A typical product from an airborne electromagnetic (AEM) survey is a conductivity depth image (CDI) along each of the flight lines. These CDIs overcome the problem of non-uniqueness by choosing one model that fits the data, typically a smoothest model. However, in the case of using AEM for describing the stratigraphy of the regolith, an understanding of the landscape evolution processes that formed the regolith gives us knowledge about what the stratigraphic units are that make up the regolith, and also something about their likely geometry. In addition, knowledge of their mineralogy tells us something about their likely ranges of conductivity, and understanding of the processes that formed them tells us about their geostatistical properties. For example, materials which are well mixed, such as channel clays, will typically be homogeneous over large distances, whereas material that has formed by in-situ weathering could be much more heterogeneous. It therefore makes sense to try to invert the AEM data for stratigraphic boundaries and conductivity variations within stratigraphic units rather than smooth models. This immediately gives estimates, with uncertainty bounds, for the depths to various interfaces, which are of more direct interest to a geologist than the conductivity values in the CDI.

The work presented here shows how the use of geological contextual information can produce improved inverted models of the regolith vertical and lateral stratigraphy from AEM data. A better understanding of regolith architecture then allows for optimisation of drilling sites for geochemical sampling, focussing on stratigraphic units where the geochemical footprint of an orebody is likely to have been concentrated.

**Key words: Inversion, Airborne Electromagnetics, Regolith, Landscape Evolution**

## INTRODUCTION

Regolith-dominated terrains are difficult environments for mineral exploration because of the lack of outcrop, and the fact that geochemical signatures of the basement are often masked by complex deep weathering and landscape evolution processes. (Anand and Butt, 2010; González-Álvarez et al., 2016a). Certain parts of the regolith stratigraphy may contain no expression of basement anomalies at all. However, there may be local zones where geochemical processes have concentrated the orebody footprint, and these are the sensible geochemical sampling targets. It is therefore important to understand the cover architecture in order to optimise a geochemical sampling program, and to relate geochemical anomalies in the regolith to mineral systems in the basement.

Geophysical tools are being used to assist mineral exploration in these regolith-dominated terrains. Airborne electromagnetic techniques, in particular, have been applied to mapping of groundwater and to interpreting the electrical conductivity structures within regolith (Worrall et al., 1999; Munday et al., 2001; Reid et al., 2007; González-Álvarez et al., 2016b).

A typical AEM product is a depth-conductivity section, which may consist of a set of 1D inversions of EM decays along a flight line. Each 1D inversion is non-unique — there are many models which could fit the data to within the data uncertainties — and so regularisation is often used to choose the best model; for example, using the smoothest model that fits the data to a specified amount is a common approach. We wish, instead, to use an understanding of the geology to narrow the range of acceptable solutions. An understanding of the landscape evolution tells us what sedimentary layers are expected to be present, what their stratigraphic relationships are, and something about their spatial variability. With good-enough knowledge of the regolith geology, we know what regolith layers to expect, so we invert for layer boundaries and varying conductivity within layers, rather than a general conductivity distribution.

The examples shown in this work are from the DeGrussa Copper-Gold deposit in the Bryah Basin of the Capricorn Orogen, Western Australia. The area is a regolith dominated terrain, with cover varying in thickness from less than 5m above the ore deposit to around 150m to the west. The AEM data is from a versatile time-domain electromagnetic (VTEM) survey, and information on the regolith comes from a series of borehole transects analysed by Gonzalez-Alvarez et al. (2015). We also have information on groundwater salinity and water levels from a set of water boreholes (Noble et al., 2017). Figure 1 shows a map of the flight lines and boreholes, superimposed on a time-constant image formed by fitting a single exponential decay to each sounding in the AEM survey (Sandfire Resources Ltd. Data, 2015).

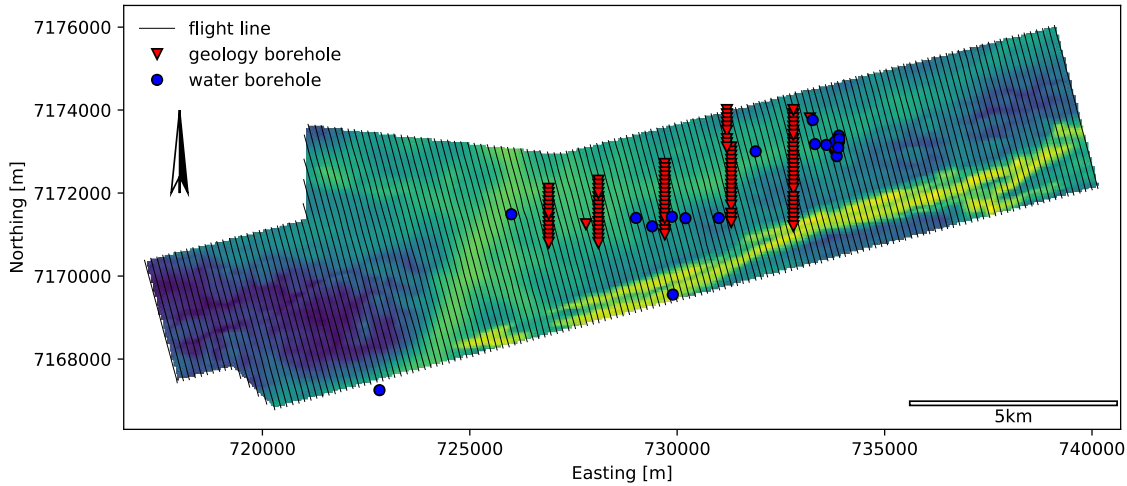


**Figure 1** Map of AEM flight lines and boreholes, superimposed on a time-constant image of the EM data. Borehole geological data after González-Álvarez et al. (2015) and water borehole data after Noble et al. (2016).

## METHOD AND RESULTS

We cast our work in a Bayesian framework (e.g. Tarantola, 1987), whereby the probability distribution for our model is composed of a prior probability, generated from our understanding of the landscape evolution based on the lateral and vertical evolution of the stratigraphy, as well as borehole information, combined with the likelihood, which is a measure of the fit to the data. The negative posterior log probability is given by

$$\log P(\mathbf{m}) \sim (\mathbf{f}(\mathbf{m}) - \mathbf{d}_{obs})^T \mathbf{C}_D^{-1} (\mathbf{f}(\mathbf{m}) - \mathbf{d}_{obs}) + (\mathbf{m} - \mathbf{m}_{prior})^T \mathbf{C}_M^{-1} (\mathbf{m} - \mathbf{m}_{prior}).$$

Here  $\mathbf{m}$  is the model parameter vector,  $\mathbf{f}(\mathbf{m})$  is the predicted data generated by our forward model,  $\mathbf{d}_{obs}$  is the observed data,  $\mathbf{C}_D$  is the data covariance matrix,  $\mathbf{m}_{prior}$  is a prior model parameter vector, and  $\mathbf{C}_M$  is the prior model covariance matrix. Our geological constraints are all incorporated into the prior parameter vector and covariance matrix. We use a 1D forward model, Airbeo (Raiche et al., 2007), for each sounding, and couple the soundings in a 2D or 3D inversion using spatial covariance in the prior. See Hauser et al. (2015) for a description of this approach.

We have a number of items of geological information that we can use to inform our AEM inversion, and that we include in the prior. We know, from analysis of borehole logs, that we are dealing with four layers: fresh basement, in-situ weathered saprolite, transported cover (channel deposits), and an overlying layer of alluvium/colluvium. We therefore parameterise our model in terms of the thicknesses and conductivities of these different layers at each AEM sounding. Previous work (King and González-Álvarez, 2016) used the known layer thicknesses at boreholes to invert nearby AEM decays for the layer conductivities, so for each layer we have a prior conductivity distribution. The prior for the resistivities includes a most-probable resistivity value for each layer (wet and dry rocks), a log-resistivity standard deviation, and an estimate of the length scale for spatial correlation, which determines the off-diagonal elements of  $\mathbf{C}_M$ .

The water table is an important feature in most geo-electrical soundings since the presence of water, especially saline water, increases

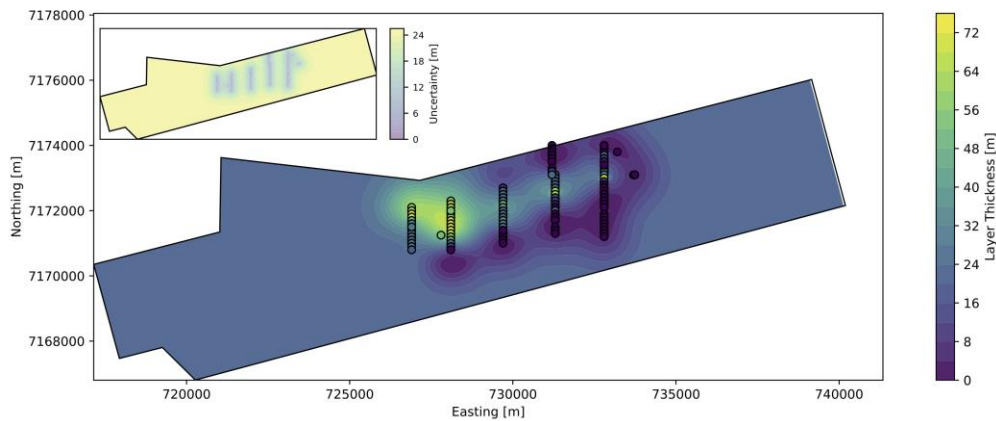


**Figure 2.** Gaussian process interpolation of transported cover (channel deposits), based on measured thicknesses at boreholes. The main image shows the expected thickness at each point, while the inset shows uncertainty, which increases with distance away from the boreholes.

the conductivity of the rock. We therefore include the water table elevation as a parameter. In our model, the water table splits a layer into wet and dry parts, each of which has its own conductivity. Water table elevations are known at water borehole locations (see Figure 1) and are interpolated using a Gaussian Process (GP) which yields an estimate of water table elevation at each sounding in the

survey, along with an uncertainty – these values are used in the prior.

Next, we have measured layer thicknesses at the borehole locations. Again, we use a GP to produce a prior mean and covariance for each of the thicknesses. Figure 2 shows an example. The layer boundary depths are determined from drilling chips, and so are only accurate to 1m. The prior uncertainty increases with distance away from the boreholes, while the most-likely thickness goes to the mean.

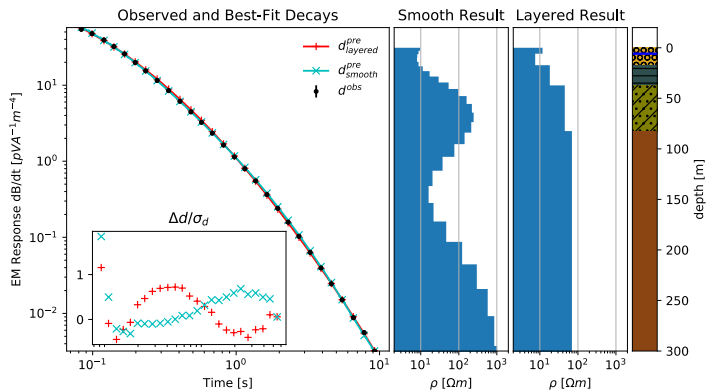


**Figure 3. Inversion results for a single sounding, comparing a smooth model to a layered model based on knowledge of the regolith. The fit to the data is similar in the two cases. On the right is a lithological display (see Figure 4 for key) of the layered inversion result, with the water level in blue. The  $\Delta d/\sigma_d$  inset shows the errors scaled by uncertainty, in an attempt to show errors that are too small to see on the main decay plot.**

section) cuts the alluvium layer into two, and over most of the section the upper, dry alluvium layer is more resistive than the wet section below the water table, as would be expected. Geological logs of nearby boreholes, which were used in forming the prior, are shown for reference. Note that the angle between the flight line and the line of boreholes means that some boreholes are closer to the line than others.

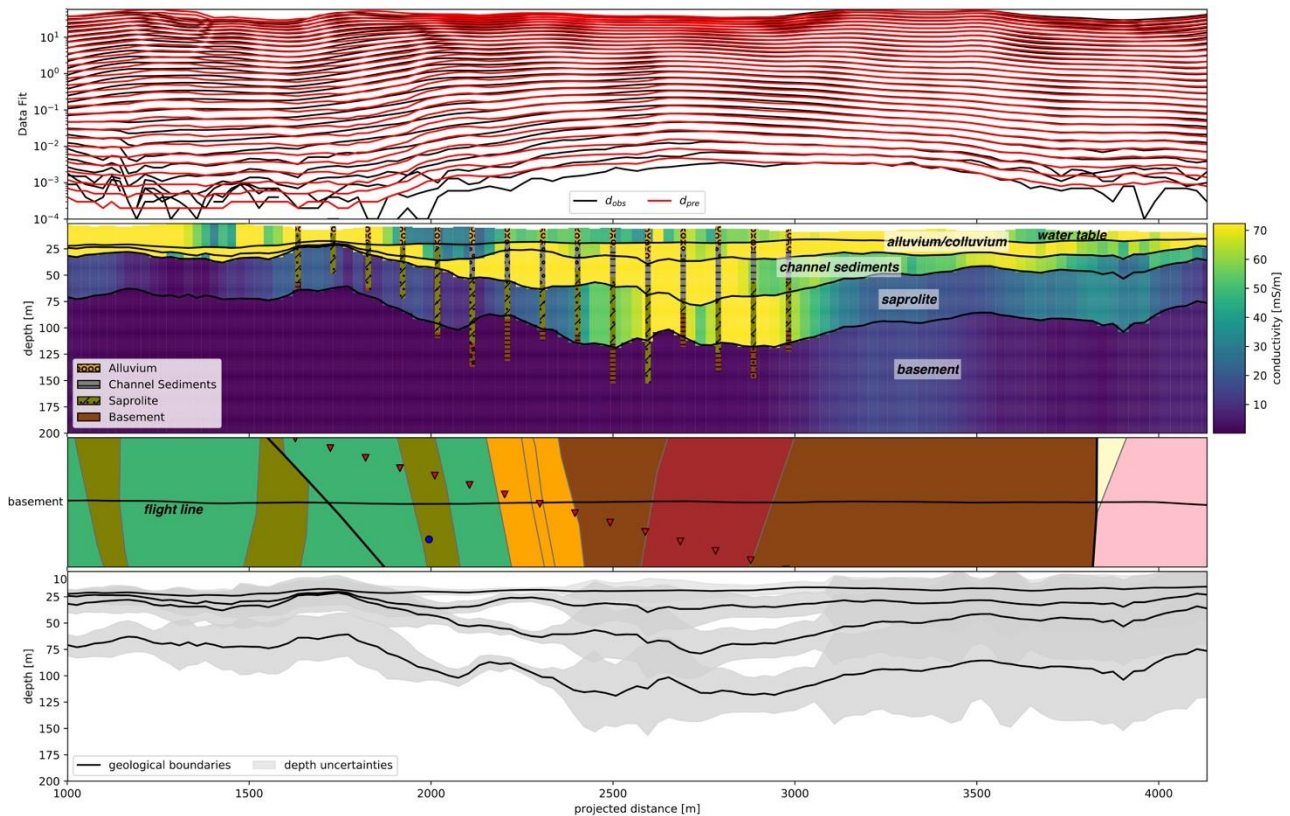


**Figure 4 An example inverted section. (a) Observed and best-fit-predicted EM data. (b) Inverted section, with nearby boreholes overlaid. (c) Plan view of interpreted basement geology, along with locations of nearby boreholes. (d) Uncertainty estimates of layer boundaries.**

### Non-uniqueness

To illustrate the phenomenon of non-uniqueness, two inversions of a sounding decay are shown in Figure 3. One inversion uses a standard, smooth model, with 30 layers. The other uses our approach, with a small number of geologically-defined layers (stratigraphic units) and the water table. The two inversions, although producing surprisingly different models, show similar fits to the observed decay curve. This means that the EM data are unable to distinguish between the two models. We believe that the layered model, being constrained by geologically-based prior information, is likely to be closer to the true geology. Note that layers picked off a conductivity-depth image based on a smooth inversion could be very different from the true geology.

An example inverted section is shown in Figure 4. The layer boundaries and the water table are indicated on the CDI by black lines. Over most of the section, the water table (the top black line on the

To give a better idea of how well our layered model corresponds to real geology, we show, in Figure 5, a layered inversion of the same line as in Figure 4, but where borehole depth information was not used. Only the average layer thicknesses over all boreholes were included in the prior – i.e. the most-likely prior model was a flat, layered one with mean thicknesses. The same prior resistivity information was included as in the previous inversion result. Clearly there is some difficulty in resolving individual layers; the channel sediments and the “wet” alluvium (below the water table) have similar conductivities. In addition, depending on the uncertainties in the data, which are not well known, there is always a trade-off between layer thickness and layer conductivity, which could be resolved with a better characterisation of the geostatistical properties of layer conductivities, their variance and spatial correlation. We have not yet included the effects of induced polarisation in the forward model, which could have a significant effect on results from this data set.

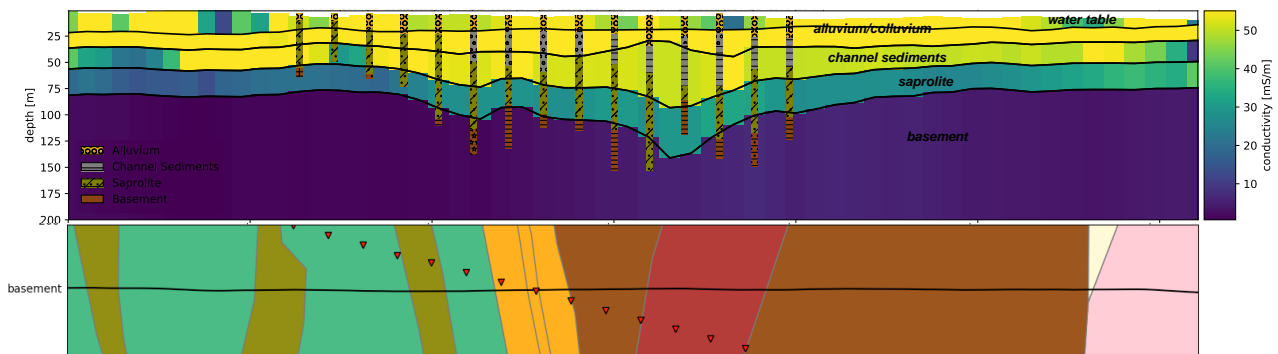


**Figure 5. A layered inversion result where no borehole depth information was included in the prior. Boreholes are plotted on the section for comparison purposes.**

## CONCLUSIONS

Instead of inverting airborne electromagnetic data for a smooth model of conductivity vs depth, we invert for the thicknesses of geological layers, which are specified based on an understanding of the regolith architecture. We have shown how a model based on known geological layering within the regolith can be used to obtain geologically-meaningful inversions of layer boundaries and their uncertainties from AEM data. The water table elevation was included in the model, and had the effect of splitting layers into wet and dry sections, each with their own conductivity. Information from geologically-logged boreholes was included into the prior by a Gaussian-process interpolation, which yielded predicted thicknesses and their uncertainties at any point in the model. The electrical conductivity distribution within each layer was constrained using values obtained by inverting AEM decays close to boreholes with known layer thicknesses. The resulting model consists of the thickness and the conductivity of each of these regolith layers at each AEM sounding over the survey area, along with the groundwater level. Rather than being a smooth conductivity image which may be difficult to interpret, the model is expressed directly in terms of geological boundaries that are of interest to an explorer.

## ACKNOWLEDGMENTS

This research was supported by the Science and Industry Endowment Fund. We would like to thank Sandfire Resources Ltd. for giving us access to the AEM dataset used in this study; and especially to Paul Hilliard.

## REFERENCES

- ANAND, R.R., AND BUTT, C. 2010. A guide for mineral exploration through the regolith in the Yilgarn Craton, Western Australia. *Australian Journal of Earth Sciences* **57**, 1015–1114.
- GONZÁLEZ-ÁLVAREZ, I., BONI, M., AND ANAND, R.R. 2016a. Mineral exploration in regolith-dominated terrains: Global considerations and challenges. *Ore Geology Reviews* **73**, 375–379.
- GONZÁLEZ-ÁLVAREZ, I., LEY-COOPER, A.Y., AND SALAMA, W. 2016b. A geological assessment of airborne electromagnetics for mineral exploration through deeply weathered profiles in the southeast Yilgarn Cratonic margin, Western Australia. *Ore Geology Reviews* **73**, 522–539.
- GONZÁLEZ-ÁLVAREZ, I., SALAMA, W., IBRAHIMI, T., AND LEGRAS, M. 2015. Palaeochannel footprint associated to DeGrussa, Western Australia. CSIRO Report, EP 158718, 87pp.
- HAUSER, J., GUNNING, J., AND ANNETTS, D. 2015. Probabilistic inversion of airborne electromagnetic data under spatial constraints. *Geophysics* **80**, E135–E146.
- KING, A.R., AND GONZÁLEZ-ÁLVAREZ, I. 2016. Integrated Inversion of Electromagnetic and Geological Data for Regolith

Characterisation. *ASEG Extended Abstracts* 1–5.

MUNDAY, T.J., MACNAE, J., BISHOP, J., AND SATTEL, D. 2001. A geological interpretation of observed electrical structures in the regolith: Lawlers, Western Australia. *Exploration Geophysics* **32**, 36–47.

NOBLE, R.R.P., ANAND, R.R., GRAY, D.J., AND CLEVERLEY, J.S. 2016. Metal migration at the degrassa Cu-Au sulphide deposit, Western Australia: Soil, vegetation and groundwater studies. *Geochemistry: Exploration, Environment, Analysis* **17**, 124–142.

RAICHE, A., SUGENG, F., AND WILSON, G. 2007. Practical 3D EM inversion - the P223F software suite. *ASEG Extended Abstracts* **2007**, 1.

REID, J., MUNDAY, T., AND FITZPATRICK, A. 2007. High-Resolution Airborne Electromagnetic Surveying for Dryland Salinity Management: The Toolibin Lake SkyTEM Case Study, W.A. *ASEG Extended Abstracts* **2007**, 1–5.

TARANTOLA, A. 1987. Inverse Problem Theory: Methods for data fitting and model parameter estimation. Society of Industrial and Applied Mathematics.

WORRALL, L., MUNDAY, T.J., AND GREEN, A.A. 1999. Airborne electromagnetics - Providing new perspectives on geomorphic process and landscape development in regolith-dominated terrains. *Physics and Chemistry of the Earth, Part a: Solid Earth and Geodesy* **24**, 855–860.